I&EC research
Industrial & Engineering Chemistry Research

pubs.acs.org/IECR

Article

Discrete Element Simulation of Gas–Solid and Gas–Liquid–Solid Flows

Jiahui Yu, Shuai Wang,* Kun Luo,* and Jianren Fan

Cite This: *Ind. Eng. Chem. Res.* 2023, 62, 17019–17028

Read Online

ACCESS | Metrics & More | Article Recommendations | Supporting Information

ABSTRACT: Multiphase flow (i.e., gas–solid flow and gas–liquid–solid flow) extensively exists in industries, yet the strong coupling between different phases poses challenges in the discrete element method (DEM)-based model establishment. This work developed a fully coupled framework by combining computational fluid dynamics (CFD) with DEM, with the further extension to incorporate volume-of-fluid (VOF) to study multiphase flow systems. A smoothing method is implemented to allow the grid size to be close to or smaller than the diameter of the particles, benefiting the subsequent interphase and interfacial interactions calculation. Iso-Advector, an advanced VOF-based surface-capturing method, is further introduced to describe interface evolution and interfacial interactions effectively. The integrated model is verified in three benchmark cases, i.e., a quasi-two-dimensional spouted bed, a fully three-dimensional spout-fluid bed, and a dam-break flow. The numerical results agree well with experimental measurements, confirming the model's reliability in simulating multiphase flow systems.

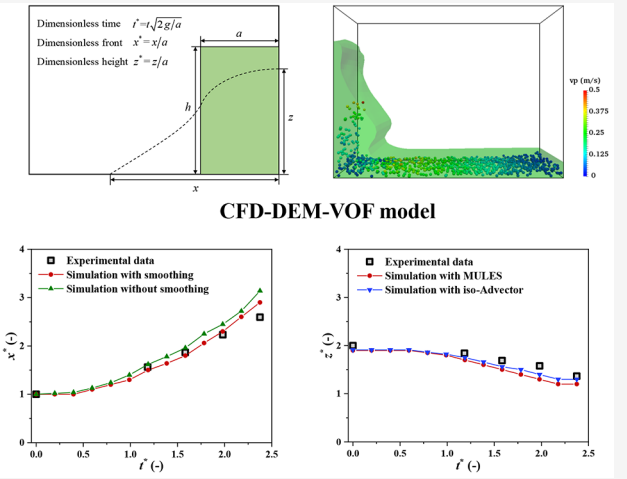

1. INTRODUCTION

Multiphase flow widely exists in chemical engineering processes including fluidized-bed drying, wet ball milling, and blast-furnace ironmaking.[1−3] The fundamental physics behind the two- and three-phase systems are the complex interparticle collisions, interphase interactions, and interfacial interactions at the particle-scale level. Over the last few decades, many experimental works have been made for a better understanding of the two- and three-phase systems.[4−6] Link et al.[5] presented a map of a spouted bed via the experimental identification of gas–solid behaviors by the positron emission particle tracking technique. Ma et al.[6] designed a gas–liquid–solid fluidized bed, where particles lighter than water were fluidized downward through the induced gas. The hydrodynamic characteristics were experimentally investigated with five types of particles under different operating conditions, and four kinds of fluidization regimes (i.e., complete fluidization, entrainment, transition, and fixed bed) were observed. Chen et al.[4] designed a bidirectional sinusoidal three-phase fluidized bed and investigated the effects of pulsed liquid frequency/amplitude and particle characteristics on the flow properties. These studies have great implications for a better understanding and design of the multiphase fluidized beds. However, the experiments are only applicable for limited operating conditions and are impractical to quantify interparticle, interphase, and interfacial interactions from the microscopic perspective.

As an alternative, numerical simulations have gained considerable attention to investigate multiphase flow.[7−11] Recently, Wang et al.[12] have conducted a comprehensive review of the applicability of numerical methods and their application in gas–solid flow simulation. The numerical methods generally consist of the Eulerian–Eulerian and Eulerian–Lagrangian methods.[13] The former regards fluid and solid phases as continuous media and simplifies interparticle collisions.[14] It is numerically efficient but has the incapability of obtaining particle information. Moreover, the complicated closures challenge the model implementation and extension.[15] On the contrary, the computational fluid dynamics discrete element method (CFD-DEM) under the Eulerian–Lagrangian framework has intrinsic advantages of fully solving interparticle collisions and accurately describing particle characteristics.[16] For the past few years, the CFD-DEM has been successfully adopted in simulating gas–solid two-phase flow in various chemical engineering processes.[17−19] Peng et al.[20] numerically studied a laboratory-scale chemical

Special Issue: MTCUE-2022

Received: April 10, 2023
Revised: June 25, 2023
Accepted: June 26, 2023
Published: August 18, 2023

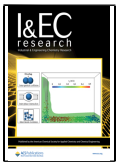

looping combustion unit using the CFD-DEM and successfully obtained flow patterns and solid distributions. Kong et al.[17] numerically studied the biomass gasification process in a bubbling fluidized bed using the CFD-DEM and thoroughly discussed the influence of key critical operating parameters on particle behavior. Besides, it is easy to develop the CFD-DEM to integrate surface-capturing models for modeling gas−liquid−solid flow involving particle−gas/liquid interactions, particle−particle/wall collisions, and gas−liquid interfacial interactions.[8] However, because of the nonlinear coupling relationship between different phases, it is still very difficult to accurately denote gas−liquid−solid systems, especially the gas−liquid interface. Furthermore, the volume-of-fluid (VOF) method is known as an efficient algorithm to capture the gas−liquid interface, extensively applied to simulate gas−liquid−solid flow.[21] A few studies have been reported on modeling gas−liquid−solid flow using the CFD-DEM coupled with VOF (CFD-DEM-VOF). Sun and Sakai[8] first developed the CFD-DEM-VOF to numerically investigate gas−liquid−solid flow, demonstrating the reasonability of VOF in capturing the gas−liquid interface. Similarly, Li et al.[22] implemented the CFD-DEM-VOF on *OpenFOAM* and tested this model by three benchmark cases, i.e., particle collision in water, particle in pure gas, and gas−liquid−solid dam break. On the basis of the same framework, Tang et al.[9] studied gas−liquid−solid behaviors and assessed the solid mixing behaviors in a rotary drum under various operating parameters. Although previous studies provide insights into the gas−solid/gas−liquid−solid flows in particulate systems, two drawbacks still need to be overcome. The first is that the grid size-to-particle diameter ratio should exceed 3 in a conventional CFD-DEM, making it difficult to accurately describe interphase interactions.[23] The second is that the conventional surface-capturing method of the MULES algorithm leads to distortion during the interface evolution.[24]

Accordingly, a well-established CFD-DEM method is extended to couple with VOF for accurate modeling of multiphase flows. The gas−liquid−solid phase interactions are denoted by a fully coupled CFD-DEM framework. The novelty of the present work can be summarized as (i) incorporating a smoothing method to allow the grid size to be smaller than the particle diameter, which benefits subsequent calculation of the interphase and interfacial interactions and (ii) implementing a recently developed iso-Advector algorithm[25] for effective capture of the interface between different phases, which is a VOF-based geometric surface reconstruction method. The paper is organized as follows: Section 2 specifies the mathematical model including governing equations, interface-capturing method, smoothing method, and numerical scheme. Section 3 verifies the accuracy of the proposed model with three benchmark cases including a quasi-two-dimensional spouted bed, a three-dimensional (3D) spout-fluid bed, and a dam-break system.

2. MATHEMATICAL MODEL

The integrated model is detailed in this section, in which the CFD module governs the fluid phase, the DEM module describes solid motions, and the VOF module captures the gas−liquid interface. A divided particle volume method is adopted to account for the contribution from the particle properties to the cell if the cell size exceeds the particle diameter. After that, a smoothing method is introduced to smooth the filtered quantities of the particle properties at the fluid cell over a length. An iso-Advector algorithm is implemented for an effective description of the interface evolution.

2.1. Fluid Phase. The volume-averaged governing equations are formulated to describe a fluid phase involving mass and momentum conservation:

$$\frac{\partial}{\partial t}(\varepsilon_f \rho_f) + \nabla\cdot(\varepsilon_f \rho_f \mathbf{u}_f) = 0 \tag{1}$$

$$\frac{\partial}{\partial t}(\varepsilon_f \rho_f \mathbf{u}_f) + \nabla\cdot(\varepsilon_f \rho_f \mathbf{u}_f \mathbf{u}_f) = \varepsilon_f(-\nabla p_f + \nabla\cdot\boldsymbol{\tau}_f + \rho_f \mathbf{g} + \mathbf{F}_s) - \mathbf{F}_{pf} \tag{2}$$

where $\mathbf{g}$ is the gravitational acceleration. ε_f, ρ_f, p_f, and $\mathbf{u}_f$ are the voidage, density, pressure, and velocity, respectively. $\mathbf{F}_{fp}$ is the interphase momentum exchange source term. $\mathbf{F}_s$ is the surface tension force. $\boldsymbol{\tau}_f$ is the fluid stress tensor, calculated as

$$\boldsymbol{\tau}_f = \mu_f \nabla \mathbf{u}_f + \mu_f (\nabla \mathbf{u}_f)^T \tag{3}$$

The VOF method is employed for capture of gas−liquid interface:[26]

$$\frac{\partial \alpha}{\partial t} + \nabla\cdot(\alpha \mathbf{u}_f) = 0 \tag{4}$$

where α ranges from 0 to 1 and can be calculated as

$$\alpha = \frac{V_{liquid}}{V_{cell} - V_{particles}} \tag{5}$$

The density (ρ_f) and viscosity (μ_f) of the gas (g)−liquid (l) mixture are formulated as

$$\rho_f = \alpha\rho_l + (1-\alpha)\rho_g \tag{6}$$

$$\mu_f = \alpha\mu_l + (1-\alpha)\mu_g \tag{7}$$

The surface tension force $\mathbf{F}_s$ is calculated by[27]

$$\mathbf{F}_s = \sigma\kappa\nabla\alpha \tag{8}$$

where σ is the surface tension coefficient. κ is the local interface curvature given by the normal vector of the gradient of α:

$$\kappa = \nabla\cdot\left(\frac{-\nabla\alpha}{|\nabla\alpha|}\right) \tag{9}$$

2.2. Solid Phase. Under the Lagrangian framework, the translational and rotational motions of particle i are calculated as[16]

$$m_i \frac{\mathrm{d}\mathbf{v}_i}{\mathrm{d}t} = m_i \mathbf{g} + \mathbf{f}_{c,i} + \mathbf{f}_{pf,i} \tag{10}$$

$$I_i \frac{\mathrm{d}\boldsymbol{\omega}_i}{\mathrm{d}t} = \mathbf{T}_i \tag{11}$$

where m_i is the mass and $\mathbf{v}_i$ is the velocity. $\mathbf{f}_{c,i}$ is the contact force, and $\mathbf{f}_{pf,i}$ is the fluid−particle interaction force. $\boldsymbol{\omega}_i$ is the angular velocity. I_i is the moment of inertia. $\mathbf{T}_i$ is the total torque. Specifically, $\mathbf{f}_{pf,i}$ can be calculated as

$$\mathbf{f}_{pf,i} = \mathbf{f}_{d,i} + \mathbf{f}_{\nabla\cdot\tau,i} + \mathbf{f}_{\nabla p,i} + \mathbf{f}_s \tag{12}$$

$\mathbf{f}_{d,i}$, $\mathbf{f}_{\nabla\cdot\tau,i}$, and $\mathbf{f}_{\nabla p,i}$ are the drag force, viscous stress force, and pressure gradient force, respectively. $\mathbf{f}_{d,i}$ is calculated by the correlation proposed by various drag models.[14,28] Specifically, the drag model for particles is mainly related to the fluid

https://doi.org/10.1021/acs.iecr.3c01173
Ind. Eng. Chem. Res. 2023, 62, 17019−17028

properties (e.g., velocity, viscosity, and density) and particle properties (e.g., velocity and diameter). The fluid properties are interpolated to the position where the particle is located. By combination with the particle properties, the drag force for each particle can be obtained. The calculation of $\mathbf{f}_{\nabla\cdot\tau,i}$ and $\mathbf{f}_{\nabla p,i}$ can refer to the previous literature.[29] The interphase force can be calculated as

$$\mathbf{F}_{\mathrm{fp},j} = \frac{1}{V_{\mathrm{cell},j}} \sum_{i=1}^{N_\mathrm{p}} w_{ij}\mathbf{f}_{\mathrm{pf},i} \tag{13}$$

where N_p is the particle number in this cell. w_{ij} is the weight identifying the contribution of the particle properties, which is given in the following section.

2.3. Interface Capturing. The gas−liquid interface needs to be well captured in the gas−liquid−solid system simulation. A suitable surface-capturing method can illustrate the interface evolution process and the resultant gas−liquid−solid behaviors. In this work, a recently developed iso-Advector algorithm is implemented to reconstruct the gas−liquid interface. Specifically, as a VOF-based geometric surface reconstruction method, the iso-Advector algorithm can capture extremely sharp interfaces.[25] The iso-Advector algorithm uses a novel interpolation scheme and can calculate the face−interface intersection evolution of cells in unstructured or structured meshes at every time step. This algorithm includes two steps: interface reconstruction and geometric advection. In the former, piecewise planar patches are constructed in each interfacial cell. The plane can cut the cell by choosing an exact volume fraction, which can be freely chosen between 0 and 1 referring to the calculation set for better calculation accuracy and efficiency. In the latter, intermediate time steps are adopted to account for the topological changes of the cell slicing along the plane movement.[25] According to the performance assessment, by validating a Rudman−Zalesak solid rotation test[30] as shown in the Supporting Information, the iso-Advector algorithm can accurately capture surface morphology.

2.4. Mapping and Smoothing. The mapping algorithm is adopted to calculate the weight w_{ij} based on the satellite point method.[23] Specifically, each particle is marked with 29 satellite points, and the weight is evaluated by division of the number of satellite points of particles in a cell by the total number of satellite points in the fluid domain. In this algorithm, the contribution from the particle to the cell only accounts for those cells that physically overlap the particle. The mapping algorithm is unsuitable for the scenario if the diameter of the particles is larger than the cell size.

To address this dilemma, a smoothing method is performed after the mapping algorithm.[31] In our previous work, the smoothing method based on the unresolved CFD-DEM is used to study the raceway dynamics, which shows advantages both in the algorithm and application perspectives.[31] The smoothing method links the quantities between the continuum phase and discrete particles by using fine grids. By solving an isotropic diffusion equation, we can obtain the smoothest variables in the computational domain. Specifically, the filtered Eulerian quantity of the particle characteristics can be smoothed over a length λ, indicating that each particle will affect the surrounding fluid at a certain distance. The smoothing length is typically specified as $\lambda = 3d_\mathrm{p}$, as suggested by the previous literature.[31] By solving the isotropic diffusion equation, the smoothing operation is achieved for transferred quantity ξ as[31]

$$\frac{\partial \xi}{\partial t} = \frac{\lambda^2}{\Delta t_{\mathrm{CFD}}}\nabla^2 \xi \tag{14}$$

The smoothing procedure is commonly performed at a small ratio of cell size-to-particle diameter ($\Delta x/d_\mathrm{p}$). When $\Delta x/d_\mathrm{p}$ is large, the mapping algorithm can deliver satisfactory results, and the smoothing procedure has no effect.

2.5. Numerical Scheme. The developed CFD-DEM-VOF model can simulate granular flow, two-phase flow, and three-phase flow. Numerical schemes for the former two scenarios have been well documented in previous publications. Thus, the coupling procedure of the last scenario is given here:

(a) The fluid field is first initialized. The free surface is then captured through the iso-Advector algorithm. After that, the mapping algorithm is adopted to calculate the weights w_{ij}, which helps to determine the contribution of the properties of particle i to cell j.

(b) After the mapping algorithm, filtered Eulerian quantities of the particle properties are available at each fluid grid and can be further smoothed over a length λ.

(c) The Eulerian fields (e.g., p_f and $\mathbf{u}_\mathrm{f}$) are transferred to the DEM module. The particle kinematics (e.g., $\boldsymbol{\omega}_\mathrm{p}$ and $\mathbf{v}_\mathrm{p}$) is then calculated based on the initial particle information and transferred fluid properties.

(d) The CFD module calls the particle information after several DEM iterations.

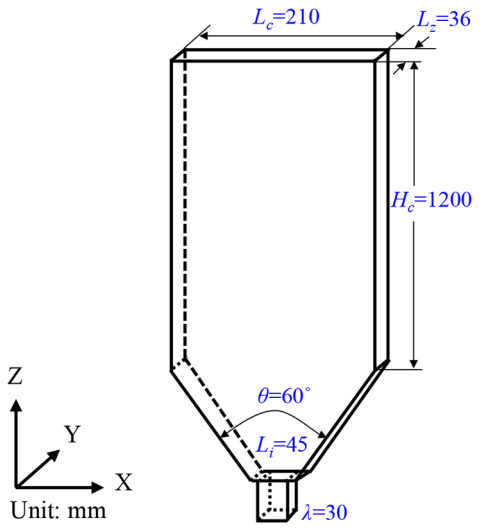

Figure 1. Schematic and the dimensions of the quasi-2D spouted bed.

Table 1. Geometry and Particle Parameters in the Simulation

parameters	value	unit
column width	210	mm
internal angel	60	deg
bottom width	45	mm
slot width	30	mm
column height	1.2	m
column thickness	36	mm
particle diameter	6	mm
particle density	2518	kg/m^3

https://doi.org/10.1021/acs.iecr.3c01173
Ind. Eng. Chem. Res. 2023, 62, 17019−17028

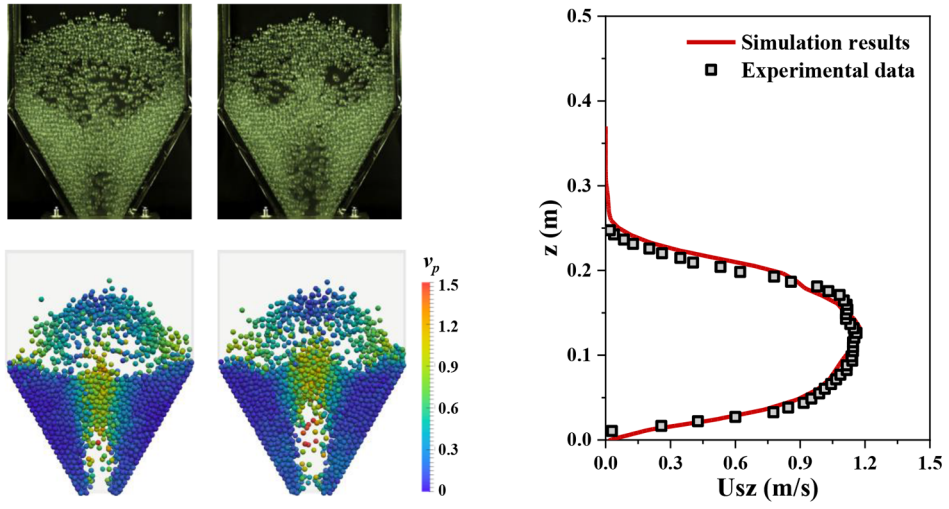

Figure 2. Comparison of the particle characteristics between the simulation results and experimental data:[34] (a) Instantaneous solid motions, where H_b = 12.4 mm and U_g = 4.39 m/s. Particles in the simulation results are colored by their velocity magnitude (v_p). (b) Solid axial velocity (Usz).[34]

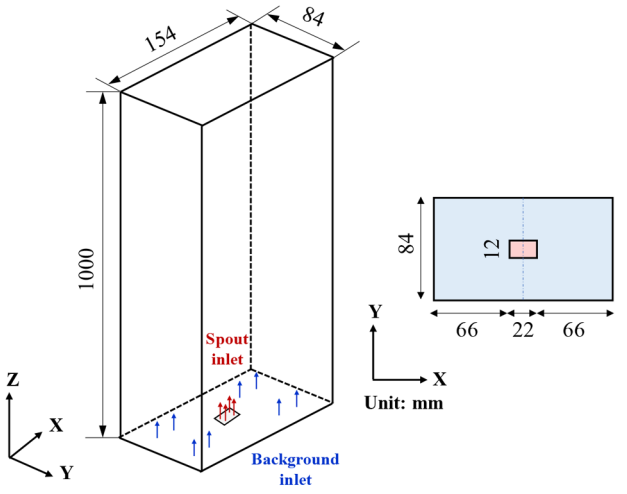

Figure 3. Schematic and the dimensions of the 3D spout-fluid bed.

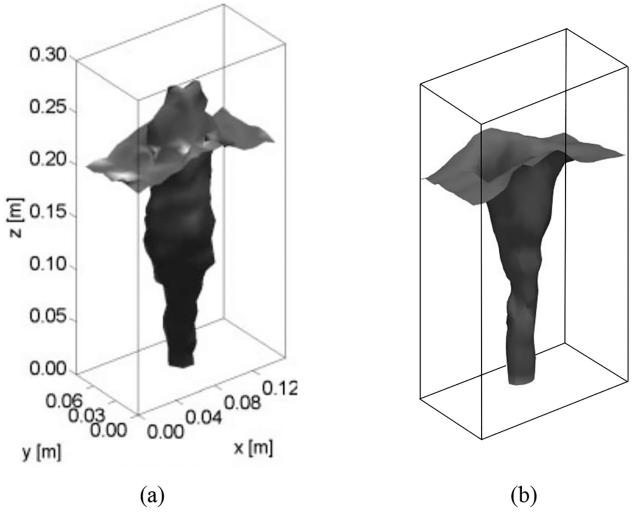

Figure 4. 3D view of the spout−annulus interface at t = 0.08 s: (a) simulation results from Link et al.;[5] (b) current simulation results.

Specifically, the fluid time step (Δt_{CFD}) should be 10−100 times larger than the solid time step (Δt_{DEM}) because a tiny Δt_{DEM} is necessary to avoid the unphysically large overlap displacement between two particles and to guarantee numerical stability.[16] Specifically, Δt_{CFD} is calculated based on the Courant−Friedrichs−Lewy (CFL) condition:[32]

$$\mathrm{CFL} = \Delta t_f \max\left(\frac{|\mathbf{u}_f|}{\Delta x}\right) < 1 \tag{15}$$

The Courant number (Co) is used in the VOF simulation:

$$Co = \frac{1}{2}\frac{\sum|\phi|}{\Delta x}\Delta t \qquad 0.01 < \alpha < 0.99 \tag{16}$$

where ϕ is the mass flux.

Δt_{DEM} is limited by the Rayleigh time (Δt_{Ray}):[33]

$$\Delta t_p = \chi \Delta t_{Ray} = \frac{\chi \pi d_p}{2(0.1631\upsilon_p + 0.8766)}\sqrt{\frac{2\rho_p(1+\upsilon_p)}{Y_p}} \tag{17}$$

where Y_p and υ_p are Young's modulus and Poisson ratio of the particles, respectively. χ is a constant in the range of 0.1−0.5, and the Δt_{DEM} is related to the particle properties.[33]

3. RESULTS AND DISCUSSION

3.1. Quasi-2D Spouted Bed from Zhang et al. (2017).

The first demonstration of the CFD-DEM model is to simulate gas−solid flow in a quasi-2D spouted bed experimentally conducted by Zhang et al.[34] Figure 1 presents the simulated geometric dimensions. Table 1 details the parameters of the geometry and the particle properties. Particles are loaded at the lower part, and the static bed height (H_b) is 12.4 mm initially. The gas is fed from the orifice, and the velocity (U_g) is 4.39 m/

https://doi.org/10.1021/acs.iecr.3c01173
Ind. Eng. Chem. Res. 2023, 62, 17019−17028

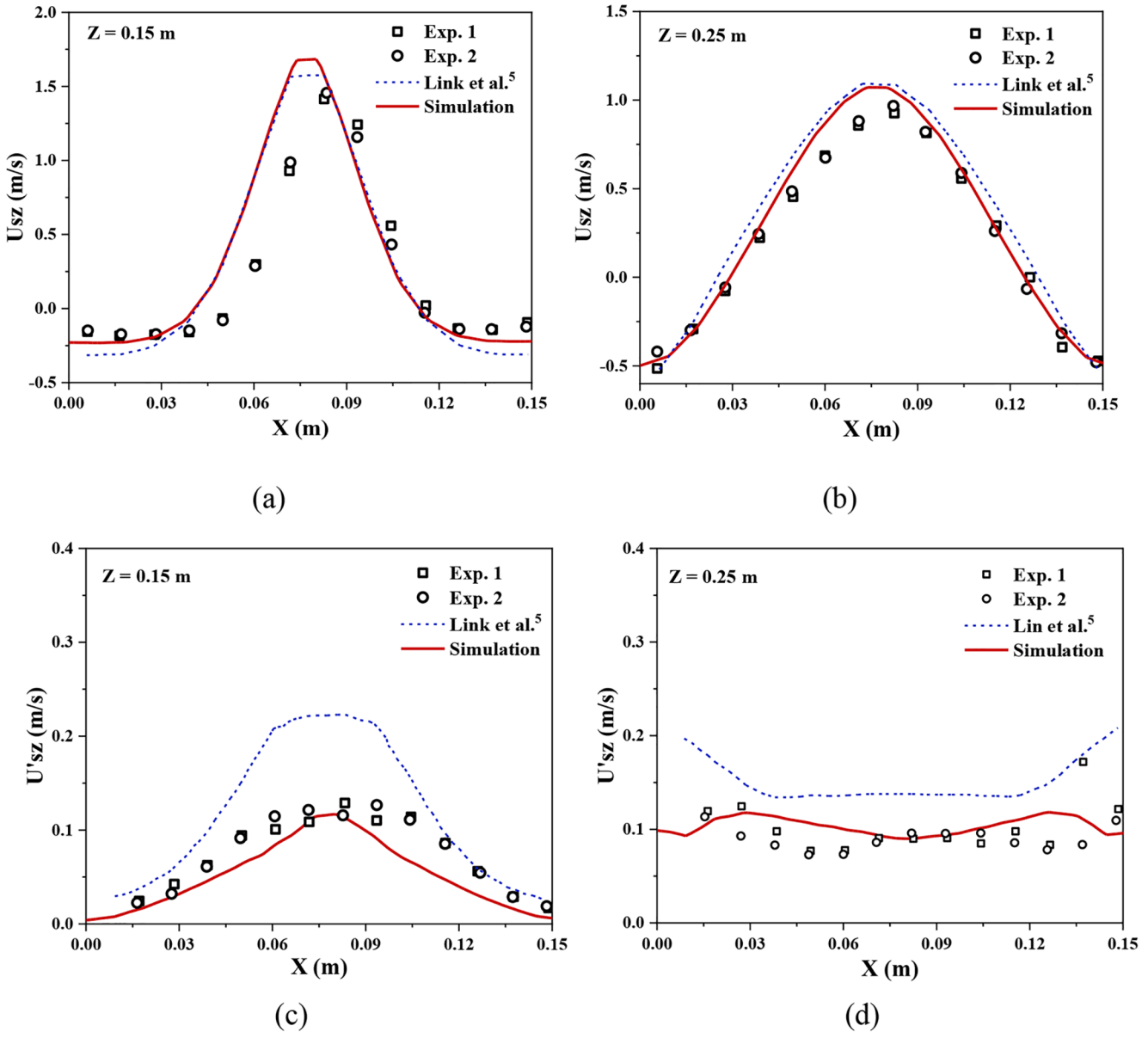

Figure 5. Comparisons of Usz with the independent simulation and experimental measurements by Link et al.[5] (Exp. 1 and 2 represent the data obtained by two independent experiments, respectively): (a) Usz at Z = 0.15 m; (b) Usz at Z = 0.25 m; (c) U′sz at Z = 0.15 m; (d) U′sz at Z = 0.25 m.

s. The right and left walls are assigned as nonslip boundary conditions, while the back and front walls are assumed as slip boundary conditions to eliminate the wall effect. The top surface is specified as the atmospheric boundary condition. The orifice is assigned as the uniform velocity inlet boundary condition.

Figure 2a compares instantaneous solid motions between the experimental and simulation results. A qualitative agreement of particle characteristics is achieved. The whole bed is generally divided into three regions, i.e., an annulus region near the sidewalls where particles move downward with low velocities dominated by the interparticle collisions, a spout region in the central bed where particles move upward with high velocities and are dominated by interphase interactions, and a fountain region with scattered particles where particles are thrown into the freeboard region. Moreover, Figure 2b compares the time-averaged vertical particle velocity (Usz) predicted using the current model and experimental data.[34] Particles accelerate rapidly from the bottom to about 0.05 m and then reach the maximum velocity (1.2 m/s) at 0.13 m due to interphase interactions. After the kinetic energy dissipation, the particles reach the maximum height of about 0.25 m. Therefore, the model can accurately predict the flow patterns and particle dynamics in quasi-2D spouted beds.

3.2. Fully 3D Spout-Fluid Bed from Link et al. (2008).

The CFD-DEM model is further demonstrated by simulating gas−solid flow in a fully 3D spout-fluid bed experimentally conducted by Link et al.[5] Figure 3 presents the geometry configuration of the invested system. The calculation domain is divided into 21, 14, and 100 in three directions. The gas is fed from the orifice with a size of 22 × 12 mm. The spout and

https://doi.org/10.1021/acs.iecr.3c01173
Ind. Eng. Chem. Res. 2023, 62, 17019−17028

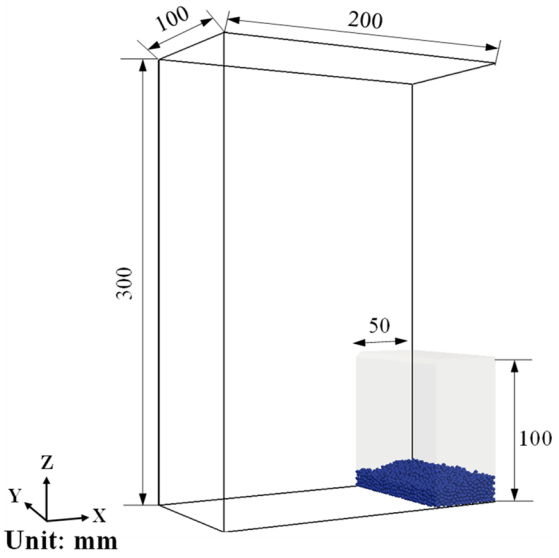

Figure 6. Schematic and the dimensions of the dam-break case.

background velocities are 60 and 2.5 m/s, respectively. The number of particles is 44800.

In 3D spout-fluid beds, the spout and annulus regions are identified by an interface. As presented in Figure 4, the 3D view of the spout−annulus interface is an isosurface with a threshold solid volume fraction of 0.3 at t = 0.08 s to differentiate different phases. It is noted that the current work can successfully reproduce the typical spout−annulus interface.

Figure 5 quantitatively compares the time-averaged vertical particle velocity (Usz) and root-mean-square (RMS) velocity (U′sz) between the current simulation and experimental data by Link et al.[5] Due to the high gas inlet velocity, a narrow spot channel characterizing the spout-fluidization regime is observed because of vigorous interphase momentum exchange intensity. Similar trends in Usz can be observed at two different heights. The current model can well reproduce vertical particle velocity with independent simulation results and experimental measurements.[5] This model better predicts the RMS velocity than the independent simulation by Link et al.[5] does. This may be caused by the fact that the soft-sphere collision model adopted in this work can more accurately describe the colliding procedure of multiple particles in dense gas−solid flow than the hard-sphere collision model used by Link et al.[5] Thus, the RMS velocity of the particles can be more accurately captured in this work. Besides, it is noted that both the current model and the model from Link et al.[5] have difficulty capturing the tendency of the RMS velocity near the wall region at Z = 0.25 m (Figure 5d), which may result from the incapability of the current drag model in reproducing gas−solid hydrodynamics near the wall region, especially for the dilute gas−solid flow. A sensitivity analysis of the existing drag models in such a scenario must be conducted in future work. In general, this model is reliable for numerical study of the particle dynamics and flow patterns in 3D spout-fluid beds.

3.3. Dam-Break Flow from Sun and Sakai (2015). The CFD-DEM-VOF model is demonstrated by simulating gas−liquid−solid flow in a dam-break case experimentally studied by Sun and Sakai.[8] The experimental observation is measured from the experimental photographs, which are recorded by a high-speed camera. As shown in Figure 6, the computational domain is 0.2, 0.1, and 0.3 m in length, depth, and height, respectively. At the initial time, a box of water is controlled by a locked door at the right corner of the computational domain with 0.05 0.1, and 0.1 m in length, depth, and height, respectively. The number of particles is 3883, and the particles with a diameter of 2.7 mm are packed at the bottom of the water. Two grid resolutions are used in this case to test the smoothing method. For coarse grids, the calculation domain is divided into 40, 20, and 60 in three directions, respectively. The $\Delta x/d_p$ value is about 1.85, suitable for the satellite point method. For fine grids, the calculation domain is divided into 80, 40, and 120 in three directions, respectively. The $\Delta x/d_p$ value is about 0.92, which is feasible for the smoothing method. Thus, the simulation with and without the smoothing method is quantitatively compared.

Figure 7 presents the particle motions and gas−liquid interface evolution during the dam-break process at different time instants. The particles are colored by the velocity magnitude. At the start time, the locked door rises, and the dam collapses at t = 0.1 s. The particles are dragged by the liquid phase due to interphase momentum exchange. The solid−liquid mixture moves to another side, forming an elongating surge front because of the accelerating water and particles. At t = 0.2 s, the liquid−solid mixture reaches the left wall and is pushed up along the wall. After t = 0.3 s, the particles fall because of the combined influence of gravity and interphase drag force. Through a comparison with the experimental data, the air−liquid interface evolution and particle motions are successfully predicted by the CFD-DEM-VOF model.

In a typical water dam process, the motion is usually described through dimensionless time t^*, waterfront position x^*, and water height z^*.[8] As illustrated in Figure 8, the waterfront position x^* and water height z^* are the normalized positions at the bottom floor and right wall, which can be calculated as[8]

$$t^* = t\sqrt{2g/a}, \quad x^* = x/a, \quad z^* = z/a \tag{18}$$

where x is the front position at the bottom floor and y is the remaining height at the right wall. a is the initial width of the dam, and t is the actual time.

Figure 9 quantitatively compares the evolution of the normalized waterfront position (x^*) and water height (z^*) over dimensionless time t^* with the experimental observations. The simulation results are in line with experimental measurements, proving the current model's applicability in predicting gas−liquid−solid flow. In the experiment, a high-speed camera is used to record the motion of the dam-break flow. At the initial time, a box of water is controlled by a locked gate at the right corner of the computational domain. It can be measured that the gate rises at a constant velocity of 0.84 m/s. Although the effect of gate rising was considered in the simulation by adding an obstacle in front of the water column, it cannot completely reflect the real effect. Thus, a slight difference can be seen in Figure 9 in that the experimental results are higher than the simulation results. Besides, the simulation with the smoothing method shows a more accurate prediction than that without the smoothing method, illustrating the necessity of the smoothing method in the gas−solid-flow system simulation.

Accordingly, the advanced interface-capturing method of the iso-Advector algorithm[25,35] is implemented and compared with the conventional MULES algorithm in predicting the dimensionless waterfront position and water height at three

https://doi.org/10.1021/acs.iecr.3c01173
Ind. Eng. Chem. Res. 2023, 62, 17019−17028

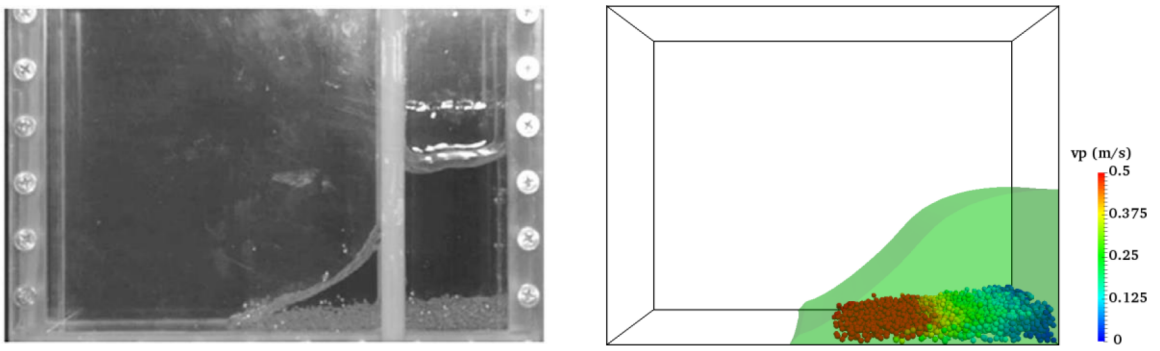

(a) $t = 0.1$ s

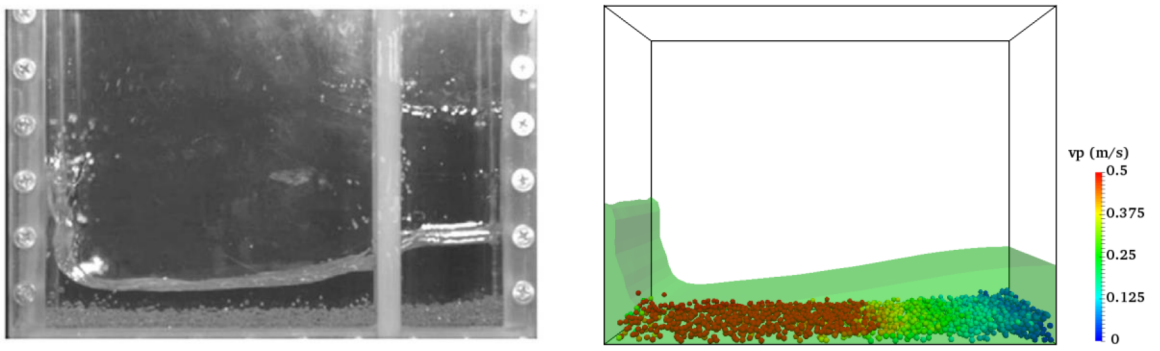

(b) $t = 0.2$ s

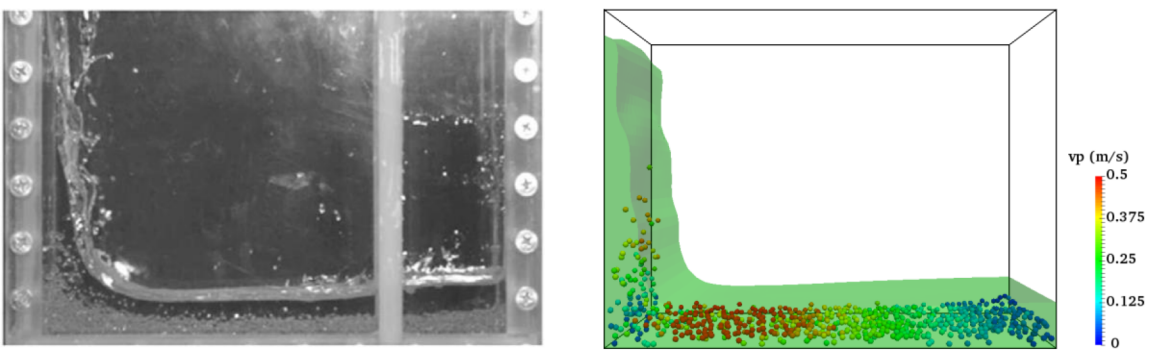

(c) $t = 0.3$ s

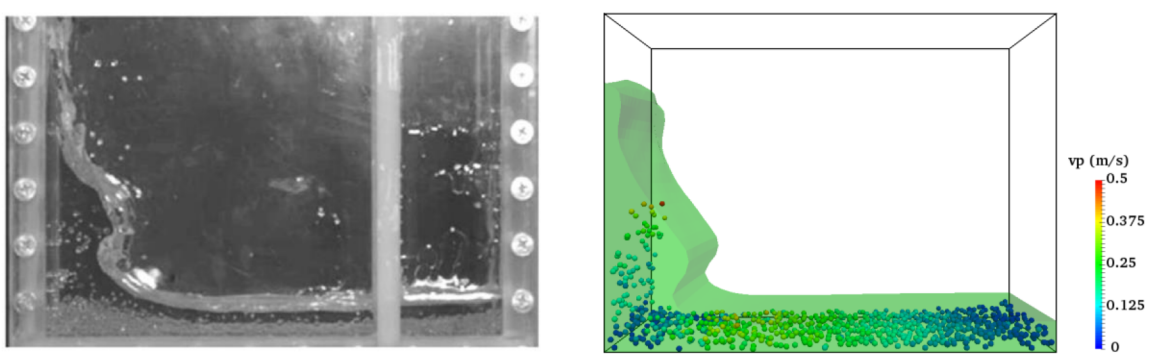

(d) $t = 0.4$ s

Figure 7. Comparisons of the predicted particle motions and gas−liquid interface evolution (right column) with experimental observations (left column)[8] at different time instants: (a) $t = 0.1$ s; (b) $t = 0.2$ s; (c) $t = 0.3$ s; (d) $t = 0.4$ s. Particles in the simulation results are colored by the velocity magnitude (v_p).

https://doi.org/10.1021/acs.iecr.3c01173
Ind. Eng. Chem. Res. 2023, 62, 17019−17028

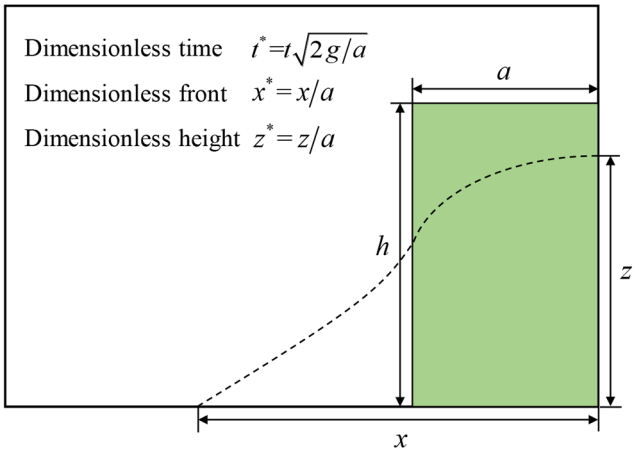

Figure 8. Schematic diagram and calculation procedure of the normalized variables in a typical dam-break process.

typical time instants. As illustrated in Figure 10, the iso-Advector algorithm can more accurately predict the interface evolution than the MULES algorithm in the dam-break benchmark case, indicating the superiority of the iso-Advector algorithm in modeling gas−solid−liquid systems.

4. CONCLUSION

In this study, a fully coupled framework by combining CFD with DEM is developed, with a further extension to incorporate VOF to study gas−solid and gas−liquid−solid flows. The integrated model is verified in three benchmark cases, i.e., a quasi-2D spouted bed, a fully 3D spout-fluid bed, and a dam-break flow. Tips are given by the following:

(1) The interactions between gas/liquid−solid phases are denoted through a fully coupled CFD-DEM framework. The VOF method is adopted to describe the free surface and update the fluid properties and liquid volume fraction. Furthermore, a smoothing method is implemented to allow

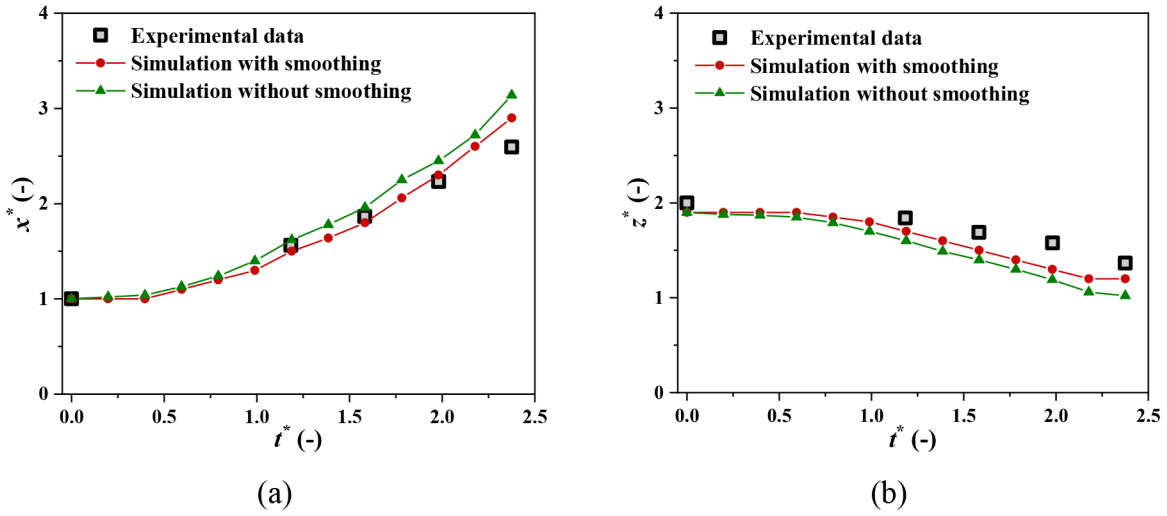

Figure 9. Comparisons of the predicted normalized waterfront position x^* (a) and water height z^* (b) over dimensionless time with the experimental observations.[8] The surface-capturing method of the MULES algorithm is used in the two scenarios to assess the smoothing method.

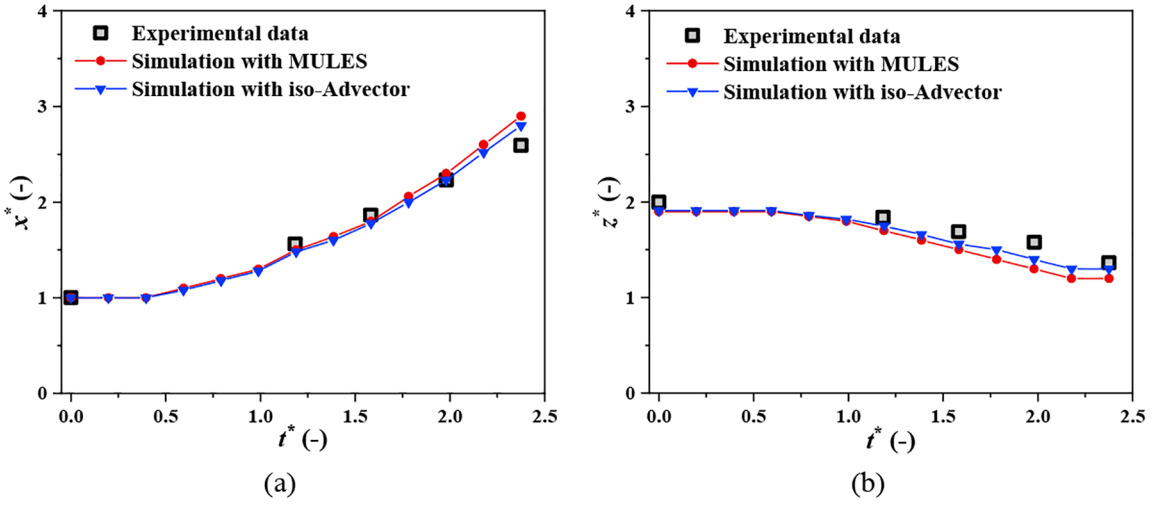

Figure 10. Comparisons of the predicted normalized waterfront position (a) and water height (b) over time with the experimental observations.[8] The smoothing method is used in the two scenarios to assess the iso-Advector algorithm.

https://doi.org/10.1021/acs.iecr.3c01173
Ind. Eng. Chem. Res. 2023, 62, 17019−17028

the size of the grid to approach or be smaller than the diameter of the particle, better for the subsequent calculation of the interphase and interfacial interactions. Iso-Advector, an advanced VOF-based surface-capturing method, is further introduced to effectively describe the interface evolution and interfacial interactions.

(2) The current model can well reproduce the vertical particle velocity and RMS velocity in spout-fluid beds, which indicates its reliability to predict the flow patterns and particle dynamics in spout-fluid beds. In the dam-break flow simulation, the air−liquid interface evolution and particle motions are successfully captured by the CFD-DEM-VOF model. Besides, this work considering a smoothing method shows a more accurate prediction than that without a smoothing method, indicating the need for a smoothing method in gas−solid-flow system simulation. Compared with MULES, the iso-Advector algorithm can more accurately predict the interface evolution in the dam-break benchmark case, indicating the superiority of iso-Advector in modeling gas−solid−liquid systems.

Thus, this work provides an accurate and reliable integrated model for numerical study of gas−solid and gas−liquid−solid flows.

■ ASSOCIATED CONTENT

Supporting Information

The Supporting Information is available free of charge at https://pubs.acs.org/doi/10.1021/acs.iecr.3c01173.

> Comparison of the initial shape of the 2D Rudman−Zalesak solid rotation test with the shape after the rotation using different surface-capturing methods (PDF)

■ AUTHOR INFORMATION

Corresponding Authors

Shuai Wang − *State Key Laboratory of Clean Energy Utilization, Zhejiang University, Hangzhou 310027, China;* orcid.org/0000-0002-6026-2139; Email: wshuai2014@zju.edu.cn

Kun Luo − *State Key Laboratory of Clean Energy Utilization, Zhejiang University, Hangzhou 310027, China; Shanghai Institute for Advanced Study of Zhejiang University, Shanghai 200120, China;* orcid.org/0000-0003-3644-9400; Email: zjulk@zju.edu.cn

Authors

Jiahui Yu − *State Key Laboratory of Clean Energy Utilization, Zhejiang University, Hangzhou 310027, China*

Jianren Fan − *State Key Laboratory of Clean Energy Utilization, Zhejiang University, Hangzhou 310027, China; Shanghai Institute for Advanced Study of Zhejiang University, Shanghai 200120, China;* orcid.org/0000-0002-6332-6441

Complete contact information is available at: https://pubs.acs.org/10.1021/acs.iecr.3c01173

Notes

The authors declare no competing financial interest.

■ ACKNOWLEDGMENTS

We are grateful for support from the National Natural Science Foundation of China (Grant 51925603) and the Fundamental Research Funds for the Central Universities (2022ZFJH004).

■ REFERENCES

(1) Niu, L.; Huang, Y.; Chu, Z.; Cai, M.; Liu, M. Identification of mesoscale flow in a bubbling and turbulent gas-solid fluidized bed. *Ind. Eng. Chem. Res.* **2019**, *58* (19), 8456−8471.

(2) Saidi, M.; Basirat Tabrizi, H.; Grace, J. R.; Lim, C. J.; Ahmadi, G. Hydrodynamic and mixing characteristics of gas-solid flow in a pulsed spouted bed. *Ind. Eng. Chem. Res.* **2015**, *54* (32), 7933−7941.

(3) Xu, Y.; Musser, J.; Li, T.; Gopalan, B.; Panday, R.; Tucker, J.; Breault, G.; Clarke, M. A.; Rogers, W. A. Numerical simulation and experimental study of the gas-solid flow behavior inside a full-loop circulating fluidized bed: Evaluation of different drag models. *Ind. Eng. Chem. Res.* **2018**, *57* (2), 740−750.

(4) Chen, H.; Zhu, L.; Song, Y.; Liu, Z.; Wang, X.; Zhao, C.; Lu, X. Study on flow characteristics of bidirectional sinusoidal liquid pulsed gas-liquid-solid multiphase fluidized bed. *Chem. Eng. Res. Des.* **2022**, *183*, 104−117.

(5) Link, J. M.; Deen, N. G.; Kuipers, J.; Fan, X.; Ingram, A.; Parker, D. J.; Wood, J.; Seville, J. PEPT and discrete particle simulation study of spout-fluid bed regimes. *AIChE J.* **2008**, *54* (5), 1189−1202.

(6) Ma, K.; Sun, X.; Shao, Y.; Liu, M.; Zhu, J. Hydrodynamic characteristics of bubble-induced three-phase inverse fluidized bed (BIFB). *Chem. Eng. Sci.* **2019**, *209*, 115177.

(7) Mahmoodi, B.; Hosseini, S. H.; Ahmadi, G. CFD-DEM simulation of a pseudo-two-dimensional spouted bed comprising coarse particles. *Particuology* **2019**, *43*, 171−180.

(8) Sun, X.; Sakai, M. Three-dimensional simulation of gas-solid-liquid flows using the DEM-VOF method. *Chem. Eng. Sci.* **2015**, *134*, 531−548.

(9) Tang, X.; Yue, Y.; Wang, S.; Shen, Y. Modelling of gas-solid-liquid flow and particle mixing in a rotary drum. *Powder Technol.* **2022**, *409*, 117758.

(10) Wang, S.; Luo, K.; Yang, S.; Hu, C.; Fan, J. Parallel LES-DEM simulation of dense flows in fluidized beds. *Appl. Therm. Eng.* **2017**, *111*, 1523−1535.

(11) Wu, C. L.; Ayeni, O.; Berrouk, A. S.; Nandakumar, K. Parallel algorithms for CFD-DEM modeling of dense particulate flows. *Chem. Eng. Sci.* **2014**, *118*, 221−244.

(12) Wang, S.; Hu, C.; Luo, K.; Yu, J.; Fan, J. Multi-scale numerical simulation of fluidized beds: Model applicability assessment. *Particuology* **2023**, *80*, 11−41.

(13) van der Hoef, M. A.; van Sint Annaland, M.; Deen, N. G.; Kuipers, J. Numerical simulation of dense gas-solid fluidized beds: a multiscale modeling strategy. *Annu. Rev. Fluid Mech.* **2008**, *40*, 47−70.

(14) Gidaspow, D. *Multiphase flow and fluidization: continuum and kinetic theory descriptions*; Academic Press, 1994.

(15) Wang, J. Continuum theory for dense gas-solid flow: A state-of-the-art review. *Chem. Eng. Sci.* **2020**, *215*, 115428.

(16) Tsuji, Y.; Kawaguchi, T.; Tanaka, T. Discrete particle simulation of two-dimensional fluidized bed. *Powder Technol.* **1993**, *77* (1), 79−87.

(17) Kong, D.; Luo, K.; Wang, S.; Yu, J.; Fan, J. Particle behaviours of biomass gasification in a bubbling fluidized bed. *Chem. Eng. J.* **2022**, *428*, 131847.

(18) Wang, S.; Luo, K.; Fan, J. CFD-DEM coupled with thermochemical sub-models for biomass gasification: Validation and sensitivity analysis. *Chem. Eng. Sci.* **2020**, *217*, 115550.

(19) Yang, S.; Wang, H.; Wei, Y.; Hu, J.; Chew, J. W. Numerical investigation of bubble dynamics during biomass gasification in a bubbling fluidized bed. *ACS Sustain. Chem. Eng.* **2019**, *7* (14), 12288−12303.

(20) Peng, Z.; Doroodchi, E.; Alghamdi, Y. A.; Shah, K.; Luo, C.; Moghtaderi, B. CFD-DEM simulation of solid circulation rate in the

cold flow model of chemical looping systems. *Chem. Eng. Res. Des.* **2015**, *95*, 262−280.
(21) Gueyffier, D.; Li, J.; Nadim, A.; Scardovelli, R.; Zaleski, S. Volume-of-Fluid Interface Tracking with Smoothed Surface Stress Methods for Three-Dimensional Flows. *J. Comput. Phys.* **1999**, *152* (2), 423−456.
(22) Li, L.; Li, B. Implementation and validation of a volume-of-fluid and discrete-element-method combined solver in OpenFOAM. *Particuology* **2018**, *39*, 109−115.
(23) Clarke, D. A.; Sederman, A. J.; Gladden, L. F.; Holland, D. J. Investigation of void fraction schemes for use with CFD-DEM simulations of fluidized beds. *Ind. Eng. Chem. Res.* **2018**, *57* (8), 3002−3013.
(24) Gamet, L.; Scala, M.; Roenby, J.; Scheufler, H.; Pierson, J. Validation of volume-of-fluid OpenFOAM® isoAdvector solvers using single bubble benchmarks. *Comput. Fluids* **2020**, *213*, 104722.
(25) Roenby, J.; Bredmose, H.; Jasak, H. A computational method for sharp interface advection. *R. Soc. Open Sci.* **2016**, *3* (11), 160405.
(26) Hirt, C. W.; Nichols, B. D. Volume of fluid (VOF) method for the dynamics of free boundaries. *J. Comput. Phys.* **1981**, *39* (1), 201−225.
(27) Brackbill, J. U.; Kothe, D. B.; Zemach, C. A continuum method for modeling surface tension. *J. Comput. Phys.* **1992**, *100* (2), 335−354.
(28) HILL, R. J.; KOCH, D. L.; LADD, A. J. C. The first effects of fluid inertia on flows in ordered and random arrays of spheres. *J. Fluid Mech.* **2001**, *448* (448), 213−241.
(29) Zhou, Z. Y.; Kuang, S. B.; Chu, K. W.; Yu, A. B. Discrete particle simulation of particle-fluid flow: model formulations and their applicability. *J. Fluid Mech.* **2010**, *661*, 482−510.
(30) Rudman, M. A volume-tracking method for incompressible multifluid flows with large density variations. *Int. J. Numer. Methods Fluids* **1998**, *28* (2), 357−378.
(31) Radl, S.; Gonzales, B. C.; Goniva, C.; Pirker, S. In State of the art in mapping schemes for dilute and dense Euler-Lagrange simulations. *Selected Papers from the 10th International Conference on Computational Fluid Dynamics in the Oil & Gas, Metallurgical and Process Industries*; SINTEF Academic Press, 2015.
(32) Ferziger, J. H.; Perić, M.; Street, R. L. *Computational Methods for Fluid Dynamics*; Springer, 2002; Vol. 3.
(33) Wang, S.; Shen, Y. Particle-scale modelling of raceway dynamics in a blast furnace using a smoothing method. *Powder Technol.* **2021**, *389*, 189−203.
(34) Zhang, H.; Liu, M.; Li, T.; Huang, Z.; Sun, X.; Bo, H.; Dong, Y. Experimental investigation on gas-solid hydrodynamics of coarse particles in a two-dimensional spouted bed. *Powder Technol.* **2017**, *307*, 175−183.
(35) Wang, Z.; Yan, W.; Liu, W. K.; Liu, M. Powder-scale multi-physics modeling of multi-layer multi-track selective laser melting with sharp interface capturing method. *Comput. Mech.* **2019**, *63* (4), 649−661.

https://doi.org/10.1021/acs.iecr.3c01173
Ind. Eng. Chem. Res. 2023, 62, 17019−17028